TRANSPORT PROPERTIES OF DILUTE TIN-INDIUM ALLOYS

Thesis for the Degree of M. S.

MICHIGAN STATE UNIVERSITY

Richard E. Fryer

1964

TRANSPORT PROPERTIES OF DILUTE TIN-INDIUM ALLOYS

By

Richard E. Fryer

A THESIS

Submitted to
Michigan State University
in partial fulfillment of the requirements
for the degree of

MASTER OF SCIENCE

Department of Physics and Astronomy
College of Natural Science

1964

ABSTRACT

TRANSPORT PROPERTIES OF DILUTE
TIN-INDIUM ALLOYS

by Richard E. Fryer

Five alpha phase tin-indium alloys, varying from 1/4% to 5% indium, were cast and drawn to .101" rods about 10cm. long. The residual resistivity and the thermal conductivity from 8°K to 30°K was measured. The thermoelectric power and the electrical resistivity of pure tin and two of the above alloys was determined from 4.2°K to 300°K. These samples for the thermopower and resistivity measurements were obtained by extruding the thermal conductivity sample into two wires, each about a meter long.

The diffusion thermopower of all samples was negative, and the pure tin sample had a large phonon drag peak at 28°K. The phonon drag term was effectively quenched with 1% solute. It is suggested that a change in the Fermi surface upon alloying is responsible for this effect.

Some of the measurements relating to thermal conductivity, or the analysis, was apparently in error, and a reliable estimate of the lattice conductivity was not obtained.

ACKNOWLEDGMENTS

I wish to thank Dr. F. J. Blatt for suggesting the problem, and for his assistance and guidance during much of this work. I also wish to express my sincere appreciation to Dr. Peter A. Schroeder for his encouragement and suggestions concerning interpretation of the data.

Financial support by the Atomic Energy Commission is gratefully acknowledged.

TABLE OF CONTENTS

LIST OF TABLES

LIST OF FIGURES

I. INTRODUCTION

To gain an understanding of the properties of conduction electrons in a metal, several methods of getting detailed information about the Fermi surface have been devised. Many of these methods are only useful in the cases of extremely pure metals and low temperatures. Transport effects are not restricted to these conditions, however. Thermal conductivity, electrical conductivity, and thermoelectric power are transport properties which are sensitive to variations in the properties of conduction electrons, and they are theoretically related.

The object of this thesis is to (1) describe the two apparatus and the methods used to measure the above transport properties, and (2) describe and analyze the results of those measurements.

II. Theory

Thermoelectric power

If a temperature gradient is set up in a metal, electrons will instantaneously flow towards the cold end. A potential difference builds up between the ends of the metal until the current produced by the temperature gradient is balanced by an equal and opposite current produced by the EMF. If the temperature at one, T_1, is fixed, and the other, T_2, is varied, the derivative of the EMF with respect to T_2 is called the thermopower of the metal at temperature T_2:

$$S = \frac{d\ (EMF)}{dT} \qquad \text{Eqn. 1.}$$

If a thermocouple is made of two different metals, such as in Fig. 1, then Jones (1956) shows:

$$EMF = \int_{T_1}^{T_2} (S_B - S_A)\ dT \qquad \text{Eqn. 2.}$$

where S_A and S_B are the characteristic thermopowers of metals A and B respectively. If T_1 is held constant, then:

$$\frac{d(EMF)}{dT_2} = S_{AB} = S_B(T_2) - S_A(T_2) \qquad \text{Eqn. 3.}$$

where S_{AB} is the thermopower of the two metal thermocouple combination. If the wires (metal B) and the sample (metal A) are the same material, Eqn. 3 shows that the EMF will not vary with termperature. In fact, it will be zero.

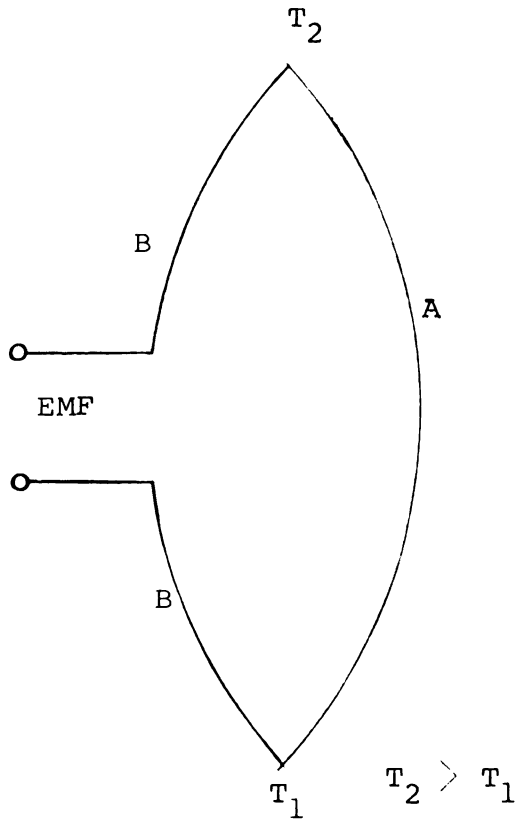

Figure 1. Schematic of alloy - lead thermocouple assembly.

An experimental measure of the thermopower of the alloy, wire A, is then possible if the thermopower of metal B is known.

If the thermopower is derived considering only that some mechanism exists that can re-establish the electron distribution once it has been disturbed, but ignoring any effects due to the drift velocity of phonons, then the result is called the diffusion thermopower, and Wilson (1954) shows that this has the form:

$$S_d = \frac{2}{3e} K^2 T \left\{ \frac{\partial}{\partial E} [\log \sigma(E)] \right\}_{E = \zeta} \qquad \text{Eqn. 4.}$$

Where K is the Boltzman constant, $\sigma(E)$ is electrical conductivity of the metal, ζ is the Fermi energy, and e the electron charge. This expression is valid when $T > \Theta_D$ (Θ_D is the Debye temperature) or where impurity scattering dominates (low temperature).

There is a second contribution to the thermopower due to the transport of heat by lattice vibrations. These vibrations are quantized in energy packets whose net velocity is opposite the temperature gradient. If there is an interaction between the phonons and the electrons, the flow of phonons will tend to carry, or "drag" the electrons with them from the hot to the cold end. Thus, this contribution is called phonon drag, and is denoted by S_g. The total thermoelectric power is the sum of S_d and S_g:

$$S = S_d + S_g \qquad \text{Eqn. 5.}$$

It is desirable to distinguish the terms in Eqn. 5.

Calculation of the phonon drag term involves a knowledge of phonon-electron interactions. There are two kinds of interactions, normal and Umklapp. These terms give rise to a phonon drag thermopower of opposite sign. Sondheimer (1956) shows that for pure metals at low temperatures ($T \ll \theta_D$):

$$S_g = \frac{C_q}{3Ne} \qquad \text{Eqn. 6.}$$

where C_g is lattice specific heat which varies as T^3 and N is the density of conduction electrons. This derivation neglects Umklapp process and phonon-impurity scattering.

As the temperature increases, it is necessary to look at the transfer of momentum between phonons and electrons in detail. There are two kinds of electron-phonon collisions, normal and Umklapp (U) processes. In the normal process, where $\vec{K}$ and $\vec{K'}$ are the electron wave vectors before and after collision, and $\vec{q}$ is the phonon wave vector:

$$\vec{K'} - \vec{K} \pm \vec{q} = 0 \qquad \text{Eqn. 7.}$$

Since the phonons will be traveling from the hot to cold end, they will tend to "drag" the electrons with them. As the momentum of the phonons is much smaller than the momentum of the electrons being scattered, there is a small change in momentum, and a small, usually negative, contribution to the thermopower.

In the Umklapp process, the reciprocal lattice vector, $\vec{g}$, must be included, and Eqn. 7 becomes:

$$\vec{K} - \vec{K'} \pm \vec{q} = \vec{g} \qquad \text{Eqn. 8.}$$

This results in a large change in momentum of the electron, and a correspondingly large change in S_g. In addition, the momentum reversal (which we would expect from the interpretation of a U process as a Bragg reflection) may result in a change of sign in S_g. Ziman (1961) has shown that when an extended zone is considered, distinction between normal and U processes is not necessary. He further shows that the contribution to S_g will be positive if the $\vec{q}$ vector lies in an unoccupied region of $\vec{K}$ space, and negative if it lies in an occupied region.

For alloys, impurity atoms cause considerable phonon scattering, and at high temperatures ($T \geq \theta_D$), all kinds of phonon-phonon and phonon-electron collisions will become effective. These can be suitably accounted for by an averaged relaxation time (MacDonald, 1954):

$$S_g = \frac{C_g}{3Ne} \frac{\tau_p}{\tau_p + \tau_{pe}} \qquad \text{Eqn. 9.}$$

where τ_{pe} is the average relaxation time for phonon-electron scattering, and τ_p is a relaxation time for all other events. Thus, when phonon-electron scattering dominates, $\tau_{pe}/\tau_p \ll 1$, and the low temperature limit becomes Eqn. 6. At high temperatures, $\tau_{pe}/\tau_p \gg 1$, and the equation becomes:

$$S_g \approx \frac{C_g}{3Ne} \left(\frac{\tau_p}{\tau_{pe}} \right) \qquad \text{Eqn. 10.}$$

which is proportional to T^{-1}. At room temperature in noble metals, Eqn. 10 predicts an appreciable S_g term. Instead, it is very small, possibly because the normal and U processes more or less precisely cancel each other. A detailed quantitative treatment is not possible except for monovalent metals, and even there the agreement with experiment is not complete. However, it is possible to say that the peak in S_g should appear between ($\Theta_D/5$) and $\Theta_D/10$), and is very sensitive to temperature and to the degree of distortion of the Fermi surface from a sphere. In tin, the degree of distortion is striking (Gold and Priestley, 1960).

For diffusion thermopower, Kohler (1949) has shown that:

$$S_d = \frac{\sum_j W_j S_j}{\sum_j W_j} \qquad \text{Eqn. 11.}$$

where W_j and S_j are the thermal resistivity and the thermopower of the j^{th} scattering mechanism if it alone were present. If the Wiedemann-Franz law can be validly applied to each of the thermal resistances (L_o is the Lorenz number), that is, if:

$$L_o = \frac{\rho}{WT} \qquad \text{Eqn. 12.}$$

which is true if impurity scattering dominates or if $T > \Theta_D$, then the Kohler relation can be written:

$$S_d = \frac{\sum_j \rho_j S_j}{\sum_j \rho_j} \qquad \text{Eqn. 13.}$$

which is the Nordheim-Gorter relationship. If Matthiessen's rule is obeyed:

$$\sum_j \rho_j = \rho \qquad \text{Eqn. 14.}$$

If two scattering mechanisms (a and b) are present,

$$\rho S_d = \rho_a S_a + \rho_b S_b \qquad \text{Eqn. 15.}$$

where ρ is the total resistivity and S_d is the thermopower of the alloy. In an alloy, S_a and ρ_a become the parameters of the pure metal and are associated with lattice scattering. In this case, S_b becomes the characteristic thermopower of indium in tin. Substituting ρ_b from Eqn. 14 into Eqn. 15 and dividing by ρ:

$$S_d = \frac{\rho_a S_a}{\rho} + \frac{(\rho - \rho_a)}{\rho} S_b \qquad \text{Eqn. 16.}$$

collecting terms:

$$S_d = S_b + \frac{\rho_a}{\rho} (S_a - S_b) \qquad \text{Eqn. 17.}$$

A plot of S_d against $1/\rho$, at a constant temperature, for various samples will give a linear relationship if the assumptions are fulfilled and if S_a and S_b are constants over the impurity range being considered. The intercept at $1/\rho = 0$ is S_b. Blatt (1957) shows that if the metal can be approximated as a single band of standard form, then the characteristic thermopower of the impurity in the parent metal should be proportional to T.

Electrical Conductivity

The Bloch-Gruneisen formula predicts the temperature variation of resistivity in this manner:

$$\rho = \frac{K\ T^5}{\theta^6} J_5 \left(\frac{\theta}{T}\right) \qquad \text{Eqn. 18.}$$

where $J_n(x)$ are transport integrals (Sondheimer, 1950). In the low temperature limit ($T \ll \theta$) Eqn. 18 reduces to:

$$\rho = \frac{C}{\theta} \left(\frac{T}{\theta}\right)^5 \qquad \text{Eqn. 19.}$$

And for high temperatures ($T/\theta \geq .5$):

$$\rho = \frac{C\ T}{497.6\ \theta^2} \qquad \text{Eqn. 20.}$$

The validity of this formula is dependent on the constancy of θ_D. The best approximation to this is in a pure metal, but even here there may be significant departure from the predicted temperature dependences at the low temperature limit, as it depends on the Debye temperature to the sixth power.

Matthiessen's (Jones, 1956) rule states that:

$$\rho = \rho_i + \rho_o \qquad \text{Eqn. 21.}$$

where ρ_i is the ideal resistivity, arising from scattering of electrons by phonons in the pure metal, and ρ_o is the residual resistivity, which is due to scattering of electrons by imperfections and impurities.

According to this theory, ρ_o is independent of temperature. This expression is based in part on the assumptions that: (1) The addition of impurity atoms of a different valence than the parent metal doesn't change

the effective number of electrons. (2) The impurity atoms do not affect ρ_i by changing the lattice vibrations. Neither of these approximations are likely to be strictly obeyed, so Eqn. 21 will not be exact.

Thermal Conductivity

Lattice vibrations carry heat, as can be verified by maintaining a temperature gradient in an insulating crystal. In a metal, however, conduction of heat by electrons is the dominant process. These mechanisms are essentially independent, and can be added to give the total conductivity (Klemens, 1956):

$$K = K_e + K_g \qquad \text{Eqn. 22.}$$

where K_g represents lattice conductivity, and K_e is the electronic conductivity.

In a pure metal, the thermal resistance is largely due to scattering of electrons by lattice vibrations.

Wilson (1954) has shown that this thermal resistance, called the ideal resistance, has the form:

$$W_i = \frac{4}{L_o T} \rho_{\cdot} \left[\left(\frac{T}{\cdot}\right)^5 \left\{ J_5 \left(\frac{\cdot}{T}\right) - \frac{1}{2^{\cdot 2}} J_7 \left(\frac{\cdot}{T}\right) \right\} + \frac{3 K^2 T^3}{2 Q^{\cdot 6}} J_5 \left(\frac{\cdot}{T}\right) \right] \qquad \text{Eqn. 23.}$$

where $\rho_{\cdot}$ is the resistivity at the Debye temperature, K is the Fermi radius, and Q is the Debye radius. In the limit of high temperatures, this reduces to:

$$W_i = \frac{\rho_i}{L_o T} \qquad \text{Eqn. 24.}$$

which is the Wiedemann-Franz law, and the low temperature limit is:

$$W_i = \frac{12}{\pi^2} J_5(\infty) \left(\frac{K}{Q}\right)^2 \frac{\rho_i T^2}{L_o^3} \qquad \text{Eqn. 25.}$$

At low temperatures, the residual thermal resistance can be calculated from the Wiedemann-Franz ratio. When Matthiessen's rule, Eqn. 21, is valid, the thermal resistance considering electrons only becomes:

$$W_e = W_o + W_i = \frac{\rho_o}{LT} + BT^2 \qquad \text{Eqn. 26.}$$

The coefficient of T^2 in Eqn. 25 is represented by the constant, B. In alloys, W_o is large, so K_e is small. Then K_g, the lattice conductivity, and K_e are often of comparable magnitude. If K_e can be calculated and K experimentally determined, then K_g can be found from Eqn. 22. It is not easy to measure K_g on a pure sample, for it is difficult to measure K with enough accuracy to deduce K_g reliably.

Klemens (1958) has also shown from consideration of the mean free path that K_g should vary as T^{-1} at relatively high temperatures, and as T^2 at low. At high temperatures, phonon-phonon Umklapp and phonon-impurity scattering control the conductivity; at low, phonon-electron and phonon-dislocation scattering dominates.

III. APPARATUS

Two pieces of apparatus were used in the measurements described. On the first apparatus, hereafter referred to as apparatus A, thermal conductivity measurements were made. The other apparatus, referred to as apparatus B, was used to measure thermopower and electrical resistivity.

The thermal conductivity apparatus was built by Garber, Scott, and Blatt (1963). It was originally designed with a form factor that would allow thermal conductivity, resistivity, and thermopower to be measured at the same time, using a potentiometer that was capable of measuring .01 microvolt directly. The instrument used in these measurements, a Cambridge Microstep, was limited to .1 microvolt direct measurement, thus increasing uncertainty in temperature, resistance, and thermopower by nearly an order of magnitude over previous measurements.

In Fig. 2, the heat flow, $\dot{Q}$, down the sample is given by:

$$K(T) = \frac{\dot{Q}\ \Delta L}{A\ \Delta T} \qquad \text{Eqn. 27.}$$

where ΔL is the length of the sample, ΔT the temperature between the two ends after equilibrium has been reached, and A the area. The temperature difference is maintained at 2^{o} to $3^{o}K$, and $\dot{Q}$, the power, is calculated from the voltage and current in the lower heater (T_2). The power in the upper heater (T_1) doesn't need to be measured, since it raises the temperature of the whole sample.

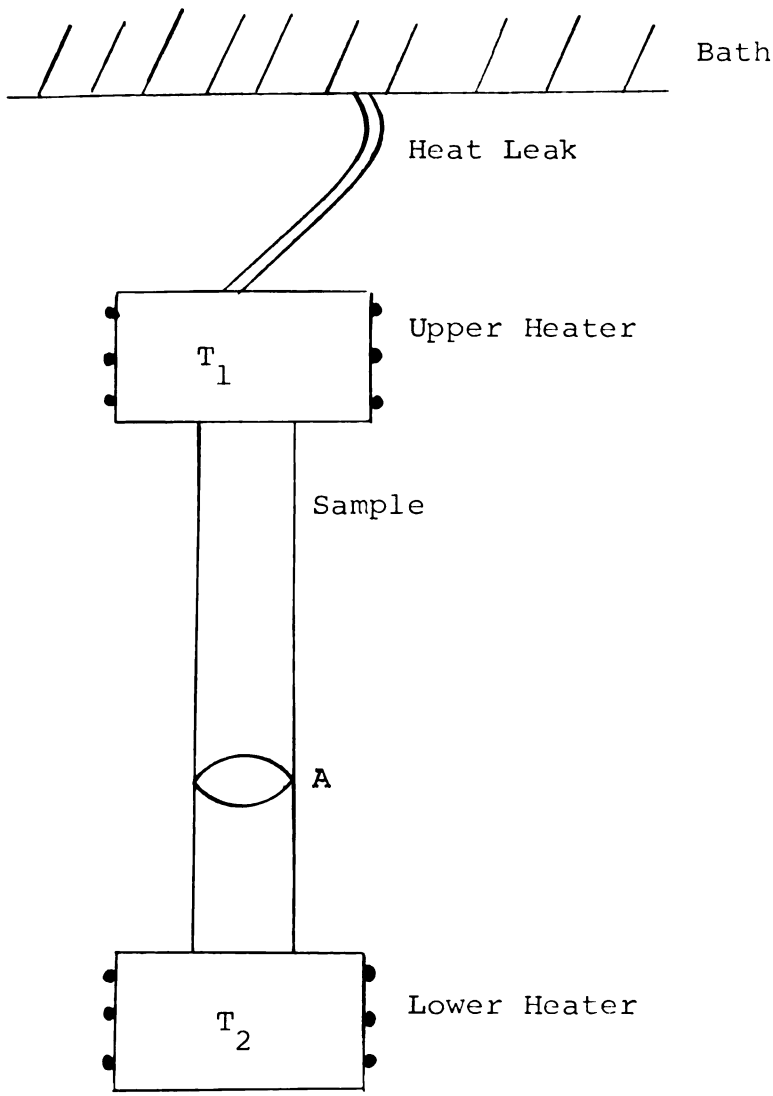

Figure 2. Schematic of thermal conductivity apparatus.

A schematic of the measuring circuits and detailed drawing of apparatus A appears in Figs. 3 and 4. The carbon resistors were not used in these measurements. A 16 lead platinum seal brings all of the electrical connections out of the vacuum can, except for the Pb potential leads, which were taken through the can directly to the copper wires in the measuring circuits by a special glass-Kovar seal. Number 36 wires were used from the seals to the outside of the dewar to minimize heat influx. The glastic rod which supports the sample, heaters, and temperature measuring plates has a very small thermal conductivity, and the upper heater block is connected via a small pure copper wire to a copper plate which is in good thermal contact with the bath. All contacts to the sample are physical, and mylar film .00024" thick used with nylon bolts provides thermal contact where electrical insulation is required. The temperature measuring plates were the location of thermocouple junctions, and were also the potential measuring points. These plates contacted the sample in a tapered opening of width 1/64" around the sample.

The heaters were wound with about 1000 ohms of manganin wire. The resistance of the leads to the heater is much less than 1000 ohms, so the power loss in the leads is much smaller than that dissipated in the heater.

A gold-2.1 at .1% cobalt vs. silver-37 at .% gold

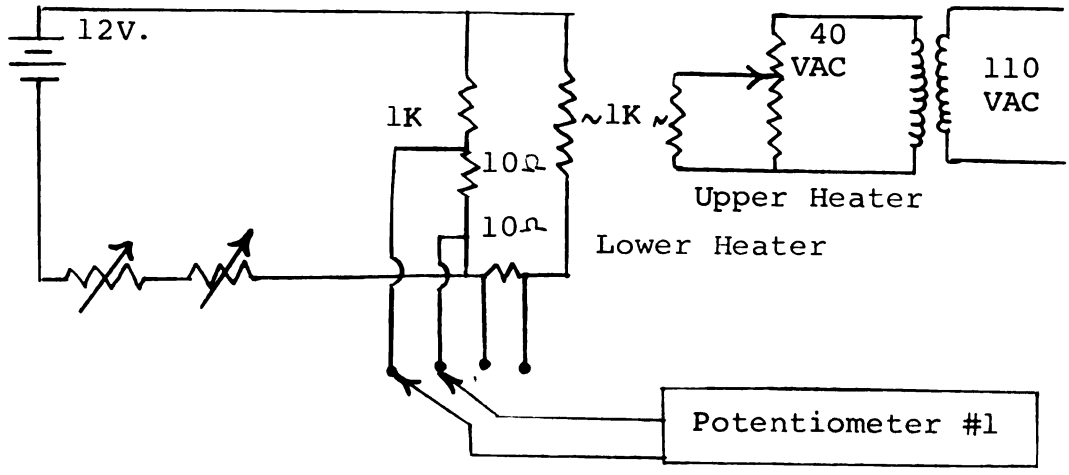

Heater Circuits

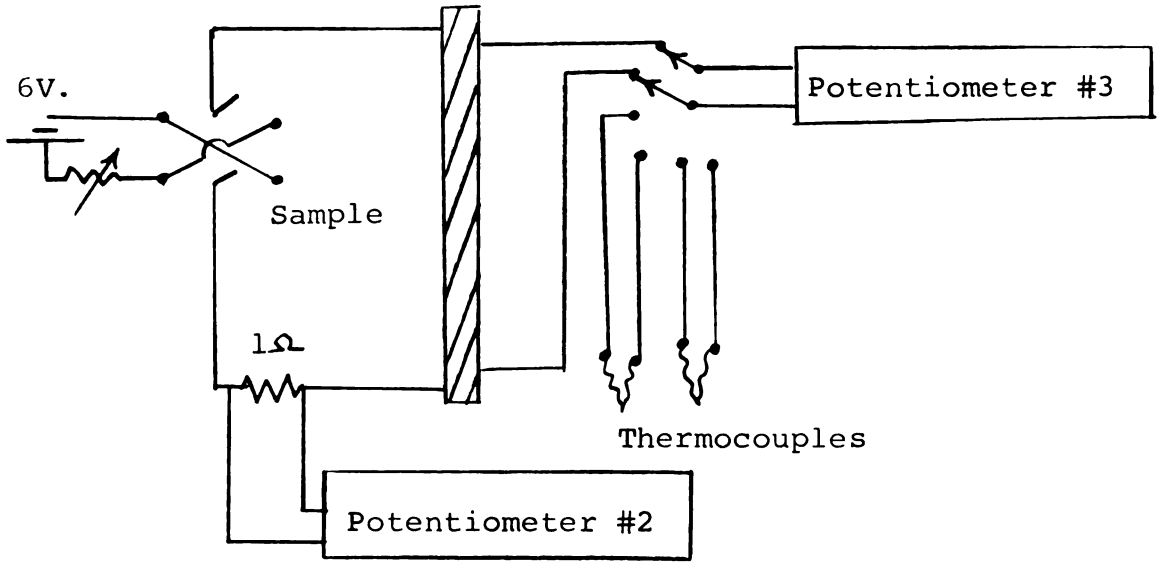

Temperature and Residual Resistance Circuit

Figure 3. Wiring diagram for apparatus A.

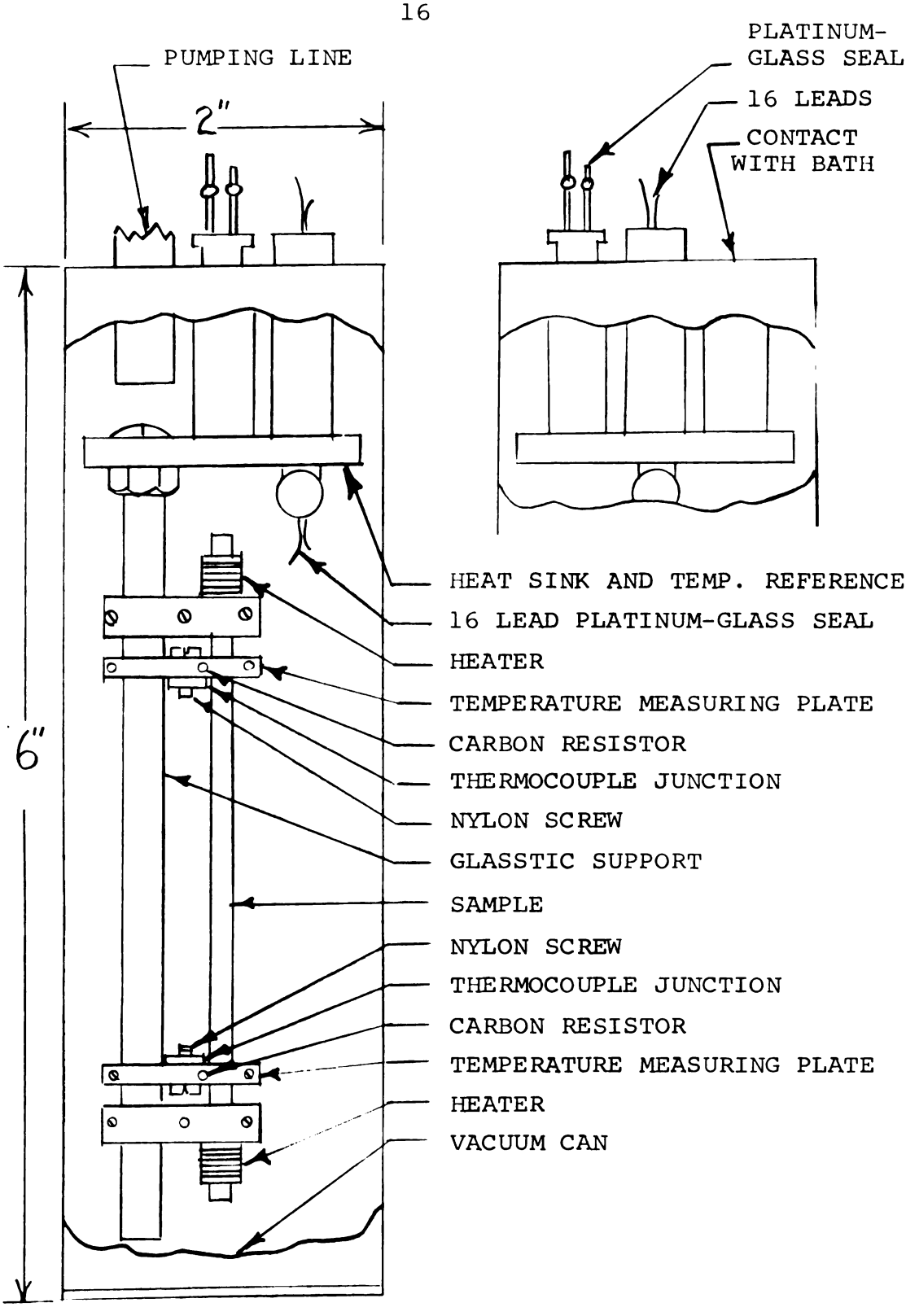

Figure 4. Apparatus A, thermal and electrical conductivity.

thermocouple is connected between the copper heat sink and the upper measuring plate, and this determines the temperature of the upper end of the sample. Another is connected between the plates, and determines the temperature difference across the sample. The thermocouple wire had been previously calibrated.

The connection of current leads for the resistance measurements is made to the copper heater block. Near liquid helium temperature the conductivity of the sample was greater than that of the heat leak. A gradient of about $2^{\circ}K$ caused the temperature of the upper end, T_1, to increase $3^{\circ}K$. This prevents an accurate measurement of the conductivity below 8° or $9^{\circ}K$.

The thermopower and resistivity cryostat, (apparatus B) was built by Wold (1963) and was designed to keep one end of the sample-Pb thermocouple at the bath temperature, and the other at a higher variable temperature. At the same time, a resistance sample was kept at this higher temperature, which could be controlled between $4.2^{\circ}K$ and $300^{\circ}K$. The apparatus consisted of the sample holder, the stainless steel support tube, and a low temperature junction which was always in the liquid.

The sample holder was a copper cylinder with holes machined in it parallel to the axis. Inserted in these were the platinum resistance thermometer and the resistance sample, mounted on a vycor rod. One end of the block was machined to a small diameter projection, on which a

manganin heater of approximately 250 ohms resistance was wound. Also, slots were turned around the block concentric with its axis to facilitate wiring changes. The base was drilled to let leads in, and then threaded to fit a copper can which enclosed all wiring connections. The other end of the stainless steel rod has a 21 pin connector, at which all electrical connections (except the heater's) are made. A styrofoam sleeve thermally insulates the can from cold gas. The apparatus is represented in Fig. 5.

To avoid discontinuities in measured voltages at low temperatures, the bismuth-cadmium eutectic (non-superconducting) solder was used for all connections to the samples. The resistivity sample and the platinum thermometer had both voltage and current leads. The cold junction of the Pb-sample thermocouple is connected to this plug, and it is interesting to note that this eleminates the need of one Pb wire, since both ends of it would be at the bath temperature. The current used for the resistance sample was 20 ma. for the alloys, 100 ma. for the pure, and 2 ma. for the platinum resistance thermometer. These currents, supplied by separate large capacity 6 volt storage batteries, were regulated by series helipot resistors, and were monitored using one ohm standards and a Leeds and Northrop type K3 potentiometer.

It was found that a stable temperature for the copper block was much more easily reached at temperatures near the bath if there was a heat leak from the copper block to the

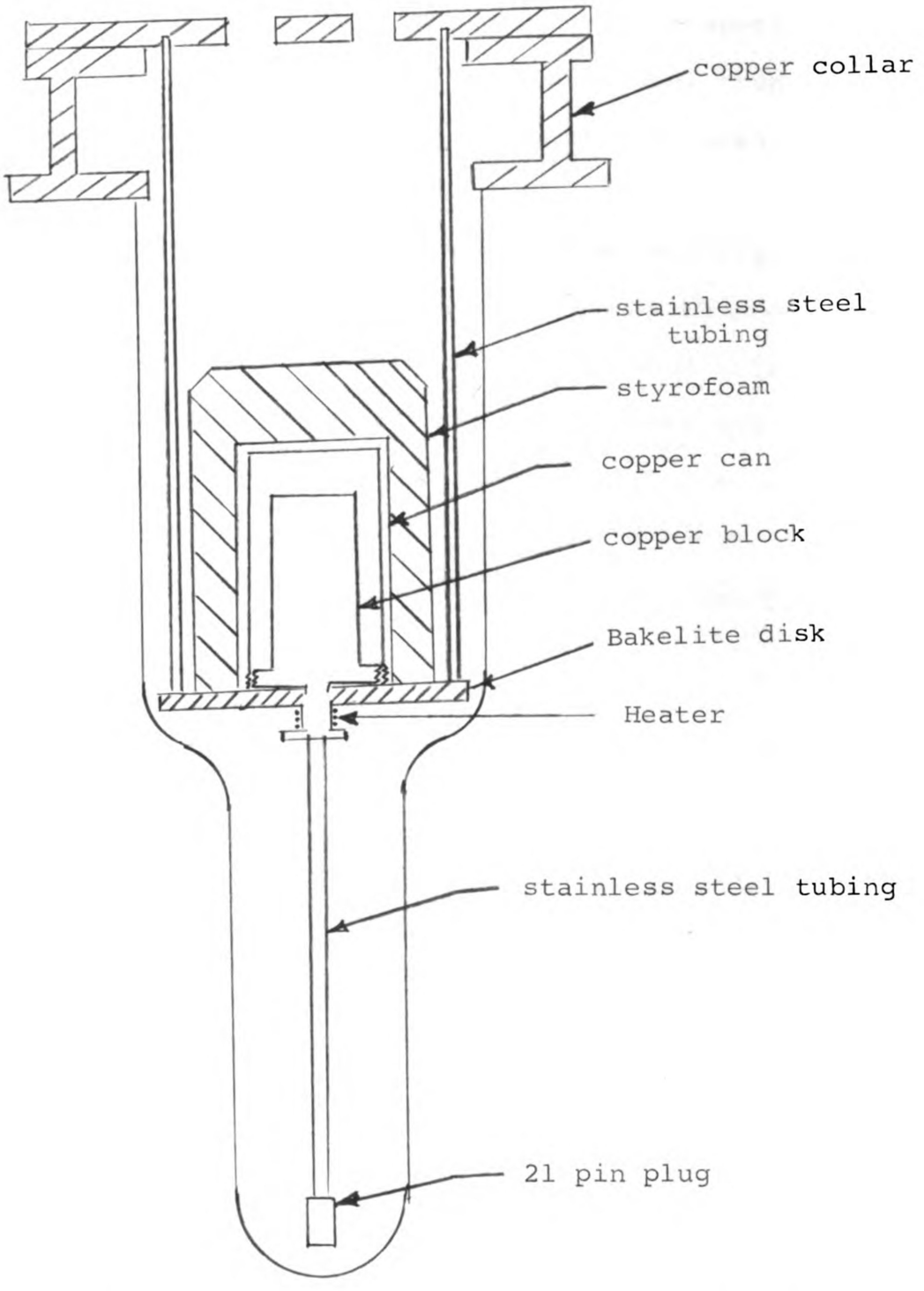

Figure 5. Apparatus B, thermoelectric power and electrical conductivity.

bath. To provide this heat leak, two number 20 wires of 7" and 11" length were connected to the block. When the block is raised to a high temperature with respect to the bath, the liquid level drops first below one, then the other wire, thereby minimizing the heat leak when it is no longer useful.

As illustrated in the wiring diagram, Fig. 6, current reversing switches were used in the thermometer and the sample circuits to eliminate voltages arising in the circuit or at the connections. The dewar was filled with liquid well up onto the block, so that the block temperature was the same as the 21 pin connector, and a preliminary check could be made of all measurements.

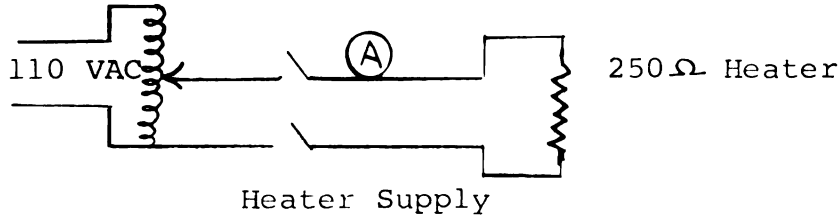

Heater Supply

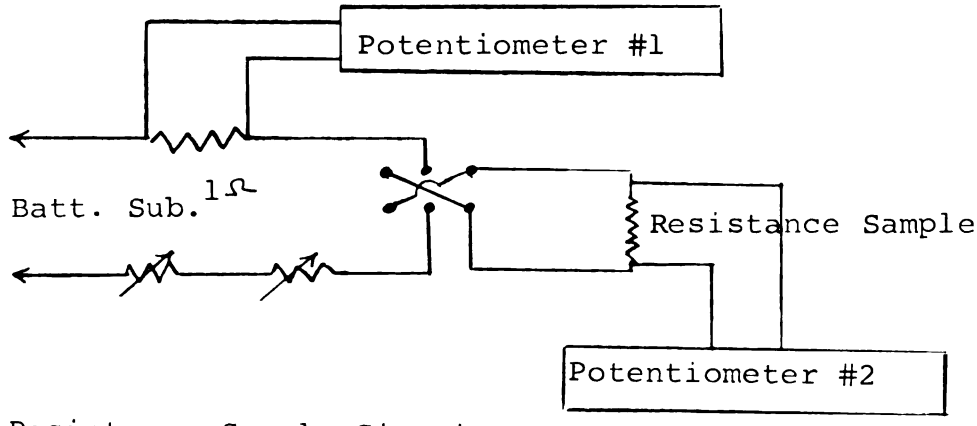

Resistance Sample Circuit

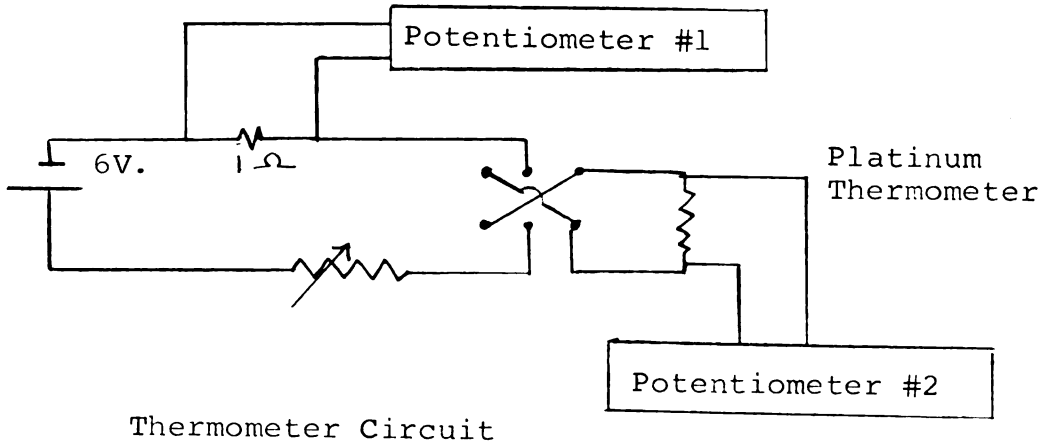

Thermometer Circuit

Figure 6. Wiring diagrams for apparatus B.

IV. PREPARATION OF SAMPLES

The pure tin sample was made from high purity (99.9999%) tin supplied by Cominco, and all alloys were made of tin (supplied by Cominco) and indium (supplied by ASARCO) of 99.999% purity. After etching in dilute HNO_3, the metals were flushed in distilled water and dried by a heat gun. They were then weighed on a Mettler balance to a precision of 10 micrograms and placed in a graphite crucible which had previously been outgassed under vacuum at temperatures above 1000°C. Then the metals were melted together, keeping the pressure below 10^{-3}mm Hg, and the crucible was agitated to facilitate mixing. The alloys were then poured into a cool cylindrical copper mold with length 2-1/2" and .150" diameter. The pour invariably wetted the copper mold near the opening, thus making a check of the loss of the metal due to evaporation impossible.

The diameter of the samples was small enough so that they could be inserted directly into a die plate, and be drawn to about .103" diameter. These samples were then heavily etched in HNO_3 to reduce them to the required .101" diameter to fit the sample holder. Five alloys (1/4%, 1/2%, 1%, 2%, 5%) were made, 8 to 10 cm. long. These were annealed in silocone oil at 185°C for about 10 hours and then slowly cooled. After the thermal conductivity measurements were made, some of these samples were

extruded through diamond dies to produce a thermopower and a resistivity specimen for apparatus B. Resistivity samples were 0.01" diameter and about 1 meter long. The thermopower samples varied in diameter (see Table 1), but all were about 1 meter long. All samples were heavily etched to remove impurities that might have entered the surface during the extruding process. The resistivity sample was wound on a 1/4" diameter by 2" vycor tube, and was sealed under vacuum into a 1/2" pyrex tube; the corresponding thermopower sample was sealed under vacuum in a 3/8" diameter pyrex tube long enough to avoid bending the sample. Then both samples were annealed for 30 hours at 185^{o}C and cooled slowly at room temperature.

Table 1. θ_o values of Sn-In samples and size of thermopower samples.

Sample (In in Sn)	Dia. Thermopower Sample	θ_o
Pure Sn	.0286"	155°K
0.99%	.0236"	145°K
2.05%	.0236"	138°K

Table 2. Residual resistivity and resistance ratios of Sn-In alloys.

Sample (In in Sn)	$\rho 273/\rho 4.2$ App. B	$\rho 4.2$, $\mu\Omega$cm App. A
5.01%	-	2.62 ± .03
2.05%	10.55	1.06 ± .04
0.99%	20.10	0.43 ± .08
0.56%	-	0.24 ± .04
0.25%	-	0.13 ± .01
Pure Sn	7150	0.00162

V. DESCRIPTION AND ANALYSIS OF RESULTS

Fermi Surface of Tin

The Fermi surface of tin has been the subject of considerable interest recently. The zone structure using a free-electron spherical Fermi surface, Fig. 7, has been worked out by Gold and Priestley (1960). Experimental resutls of several investigators agree substantially with this geometry, but Gantmakher (1963) has shown that a nearly-free electron model, based on Harrison's method, results in some improvement with his data.

Thermoelectric Power

The thermal EMF of a pure Pb-alloy thermocouple was measured as a function of the temperature (T_2 in Fig. 1) of the copper block in apparatus B. This was plotted vs. temperature and the slopes obtained by use of a mirror. This slopeis S_{AB}, the thermopower for the alloy-Pb combination. The thermopower of the alloy (or the pure metal), plotted in Fig. 8, was then obtained from Eqn. 3, using the data of Christian, et al (1958) for the thermopower of Pb.

The pure tin sample has a positive maximum of 28^{o}K, which is probably caused by phonon drag. An interpretation of the data as a positive peak superimposed on a negative diffusion component is consistent with phonon drag theory,

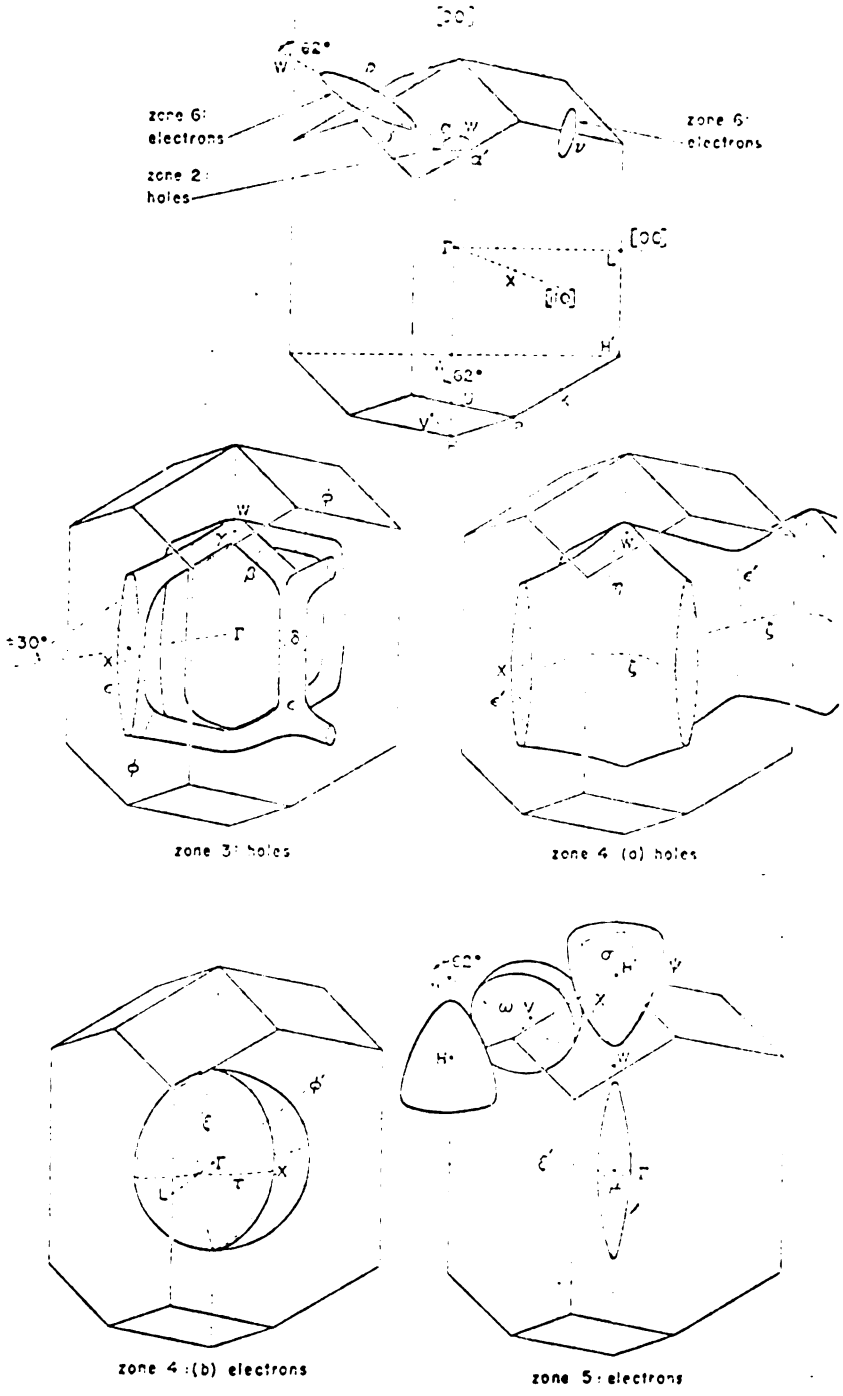

Figure 7. Fermi surface for tin.

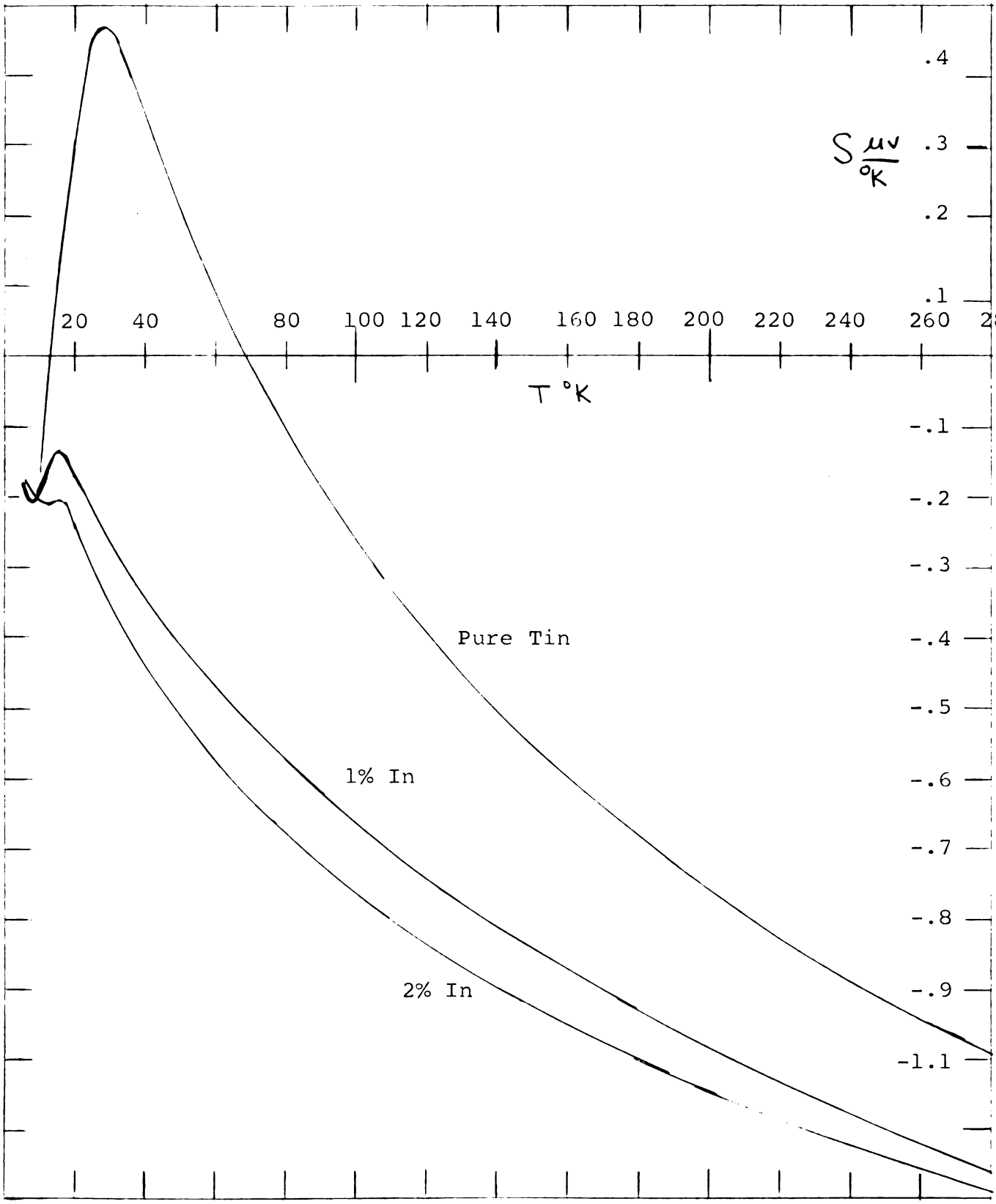

Figure 8. Thermoelectric Power of pure tin and tin-indium alloys.

and the location of the peak, about 28°K, is in the expected range. The large size of the peak is not surprising either. Inspection of the Fermi surface reveals several surfaces, particularly in zone 4, that allow scattering of electrons by phonons with q vectors lying in unoccupied regions. These processes, as pointed out previously, give a positive contribution to the phonon drag term. From 8° to 17°K, the pure tin thermopower varies approximately as T^3.

Pullan (1953) found that from 3.8° to 4.3°K, the thermopower of pure tin varied from $-T^{0.9}$ to $-T^{3.1}$, depending on crystal orientation. That is, his data was increasingly negative with temperature increase. Since the thermopower of a metal is by definition zero at 0°K, our curve must reach a minimum and go to zero. Therefore, these measurements agree with those of Pullan.

The 1% and 2% Sn-In samples had negative thermopowers at all temperatures. The addition of 1% In to Sn reduces the phonon drag peak by a large factor, and in the 2% sample, it has nearly disappeared. There are four recongized ways that the addition of a small amount of impurity can reduce the phonon drag term in this manner. In the first three, the addition of solute results in the scattering of phonons which would otherwise have contributed to the phonon drag process. In Eqn. 9, τ_{pe} becomes large and $S_g \longrightarrow 0$. The observed reduction will occur if:

(1) The solute atoms differ appreciably in mass from the

solvent. (2) The solute atoms badly distort the lattice locally. (3) The solute atoms locally distort the force constants, between adjacent atoms, resulting in modified elastic constants. (4) The Fermi surface is substantially altered by the addition of the solute atoms. In order to assess the importance of some of these factors, they are compared with the equivalent factors in the Cu-Zn results of Henry and Schroeder (1963). In the results, the phonon drag term is largely unaltered by the addition of up to 35% Zn to Cu.

The differential mass term, $\frac{\Delta M}{M}$, in Sn-In alloys is .034, and in Cu-Zn is .029. This difference cannot account for the effect. The change in lattice spacing for Sn-In alloys in the α phase is less than the corresponding change in Cu-Zn alloys (Hansen, 1958). The characteristic temperature decreased with increasing impurity, varying from 155^{o}K for Sn to 138^{o}K for 2%. The corresponding change in the Cu-Zn measurements is from 370^{o}K for pure Cu to 338^{o}K for 2.8% Cu-Zn; implies that a change in elastic constants is not responsible for the effect. I suggest then, that the drastic reduction in the phonon drag term may be ascribed to a change in the Fermi surface.

The valence of Sn is (4) and In is (3). In the periodic table, antimony, with valence (5), lies on the opposite side of Sn from In. It would be instructive to make similar measurements on tin-antimony alloys. In particular, one would see if the effect of increasing the

number of electrons in the sample also affects the phonon drag term.

The characteristic thermopower of In in Sn can be found from Eqn. 17 by plotting S_d vs. $1/\rho$. Previous measurements by Schroeder, Woolam and Wolf (to be published) on Ag-Pd and Cu-Ni alloy systems show that the characteristic thermopower of solute in solvent is accurately proportional to T, and passes through the origin. The Sn-In results, Fig. 9, show that this alloy system cannot be approximated by a single band of standard form.

Electrical Resistivity

In apparatus B, measurements were made on the resistance samples at intervals from 4.2°K to 300°K. Table 2 lists the residual resistivity and resistivity ratios, $\rho 273/\rho 4.2$, of the three samples. Kunzler and Renton, (1957) show that for pure tin samples, the size effect may be an important factor in determining the resistance ratio. If their data can be applied to this pure tin sample, the resistance ratio will be approximately 21,500, an increase by a factor of 3.1. This value of is in fairly good agreement with resistance ratios of single crystals of zone refined tin. Fig. 10 shows the variation of ρ with T for the three samples. The log of ideal resistivity, log $(\rho - \rho_o)$ is plotted vs. log T in Fig. 11 to determine the power of the temperature dependence at low temperatures, and these powers are listed in Table 3.

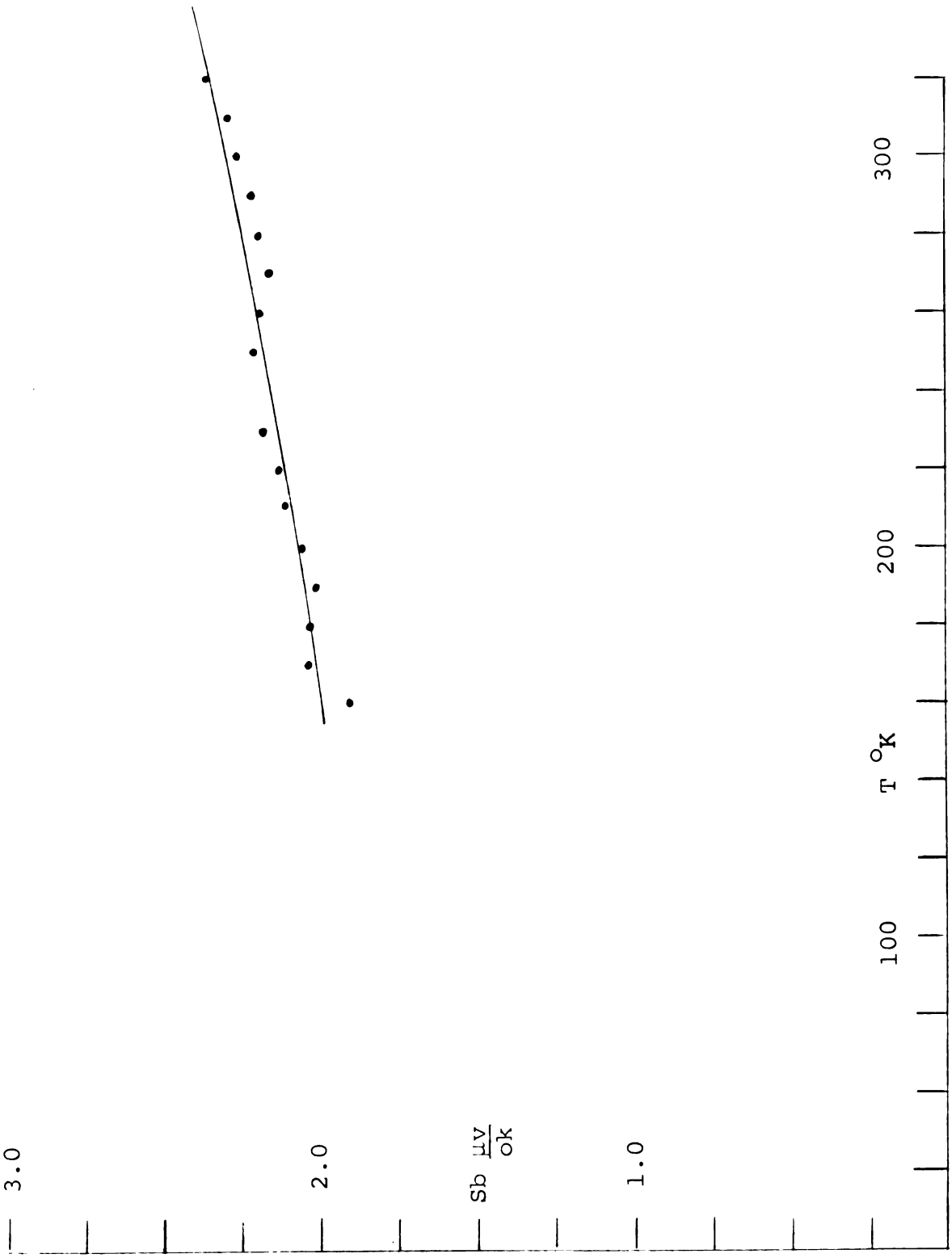

Figure 9. Characteristic thermopower of indium in tin.

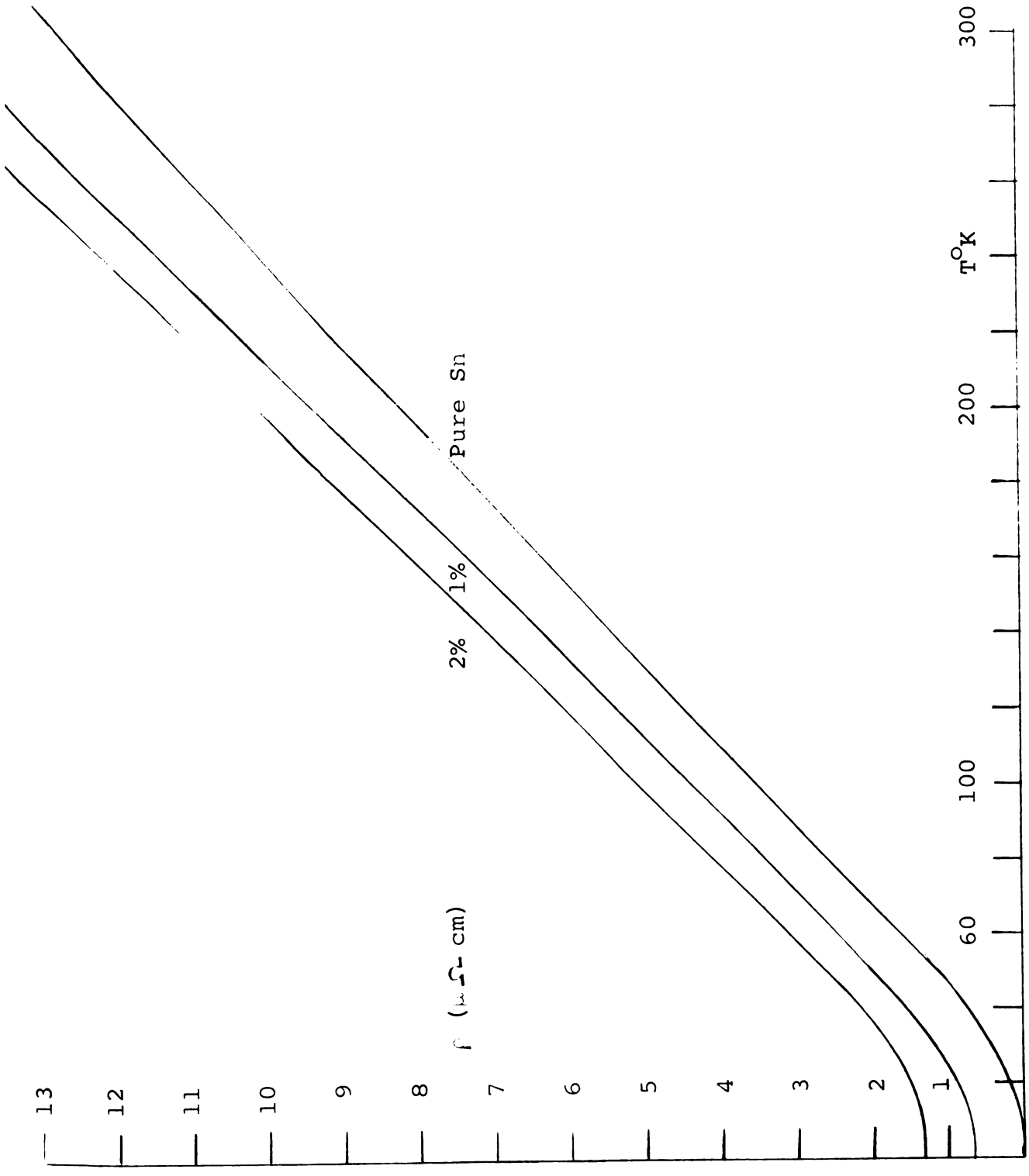

Figure 10. Resistivity of tin and tin-indium alloys.

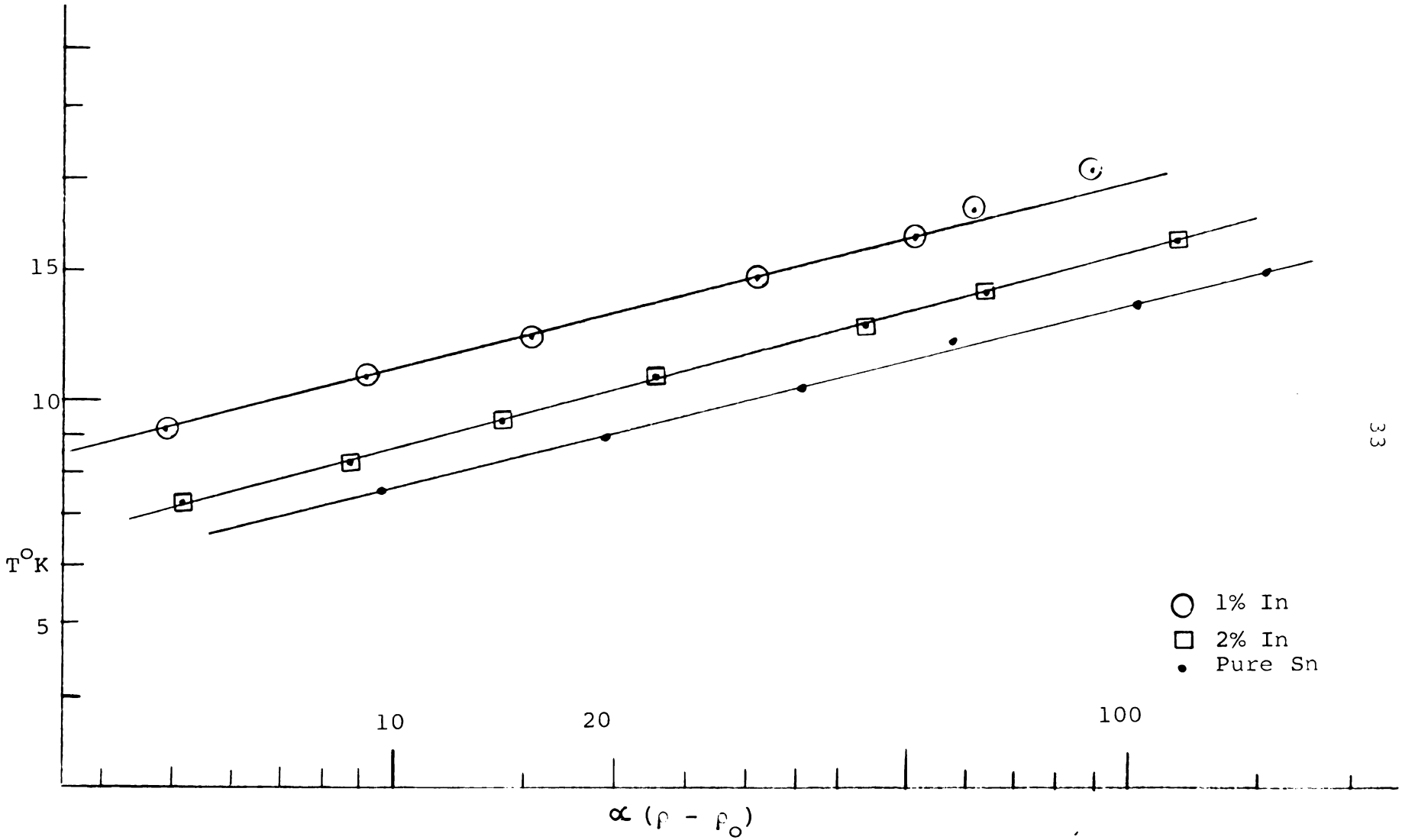

Figure 11. Log $(\rho - \rho_o)$ against log T for tin and tin-indium alloys.

Table 3. Temperature dependence of ideal resistivity curves.

Sample (In in Sn)	Slope (μ cm deg^{-1})
Pure Sn	T4.0 $\pm$ .1
0.99%	T3.6 $\pm$ .1
2.05%	T3.8 $\pm$ .1

At high temperatures ($T > \frac{\Theta}{2}$) ρ varied as T, as predicted by the Bloch-Grüneisen formula (Eqn. 20). However, at the low temperature limit, the predicted T^5 dependence (Eqn. 19) is not obeyed. Pure tin varies as $T^{4.0}$, 1% In as $T^{3.6}$ and 2% In as $T^{3.8}$. Thermal scattering is responsible for the predicted T^5 variation, and the deviation of the alloys from this law is not surprising, since the derivation is based on a number of assumptions. For pure tin, however, the $T^{4.0}$ dependence suggests that in addition to thermal scattering, at least one more temperature dependent mechanism is operating. Aleksandrov and D'Yakov (1963) find that for pure tin, the resistivity does vary as T^5, and they suggest that derivations from this in several other metals should approach the T^5 law for conditions of decreasing temperature and increasing purity. It may be that our sample would agree with the T^5 dependence at a low enough temperature.

The best fit to a theoretical Bloch-Grüneisen law was obtained by choosing various values of Θ_D and

calculating the quantity ρ/ρ_{ℓ} from the data. The θ_D which best approximated the curve at high temperature had to be reduced about 40% to fit the data near $T/\theta = .1$. This poor agreement is consistent with the T^4 resistivity variation. Some thermopower and electrical conductivity measurements were made on apparatus A, but they have considerably less precision than measurements taken with apparatus B. The results do agree qualitatively.

Thermal Conductivity

The thermal conductivity of five Sn-In alloys was measured between $8^{\circ}K$ and $30^{\circ}K$ at approximately $1\text{-}1/2^{\circ}K$ intervals. The total thermal conductivity, K is plotted against T in Fig. 12. The curves suggest that the conductivity maximum, characteristic of the pure metal, is shifted to higher temperature as the percentage of solute is increased. Shiffman (1958) made similar measurements on Sn-In alloys. Some of his results appear in several figures, and are drawn in red.

If the thermal conductivity were entirely electronic, the thermal resistivity would be given by Eqn. 26, and a plot of WT against T^3 would be a straight line with intercept $\rho_o/2$ and slope B. In a pure metal, the lattice conductivity is usually two or three orders of magnitude smaller than the electronic, and then the above approximation is valid. Going from a pure metal to an alloy, the residual thermal resistance is substantially increased, and

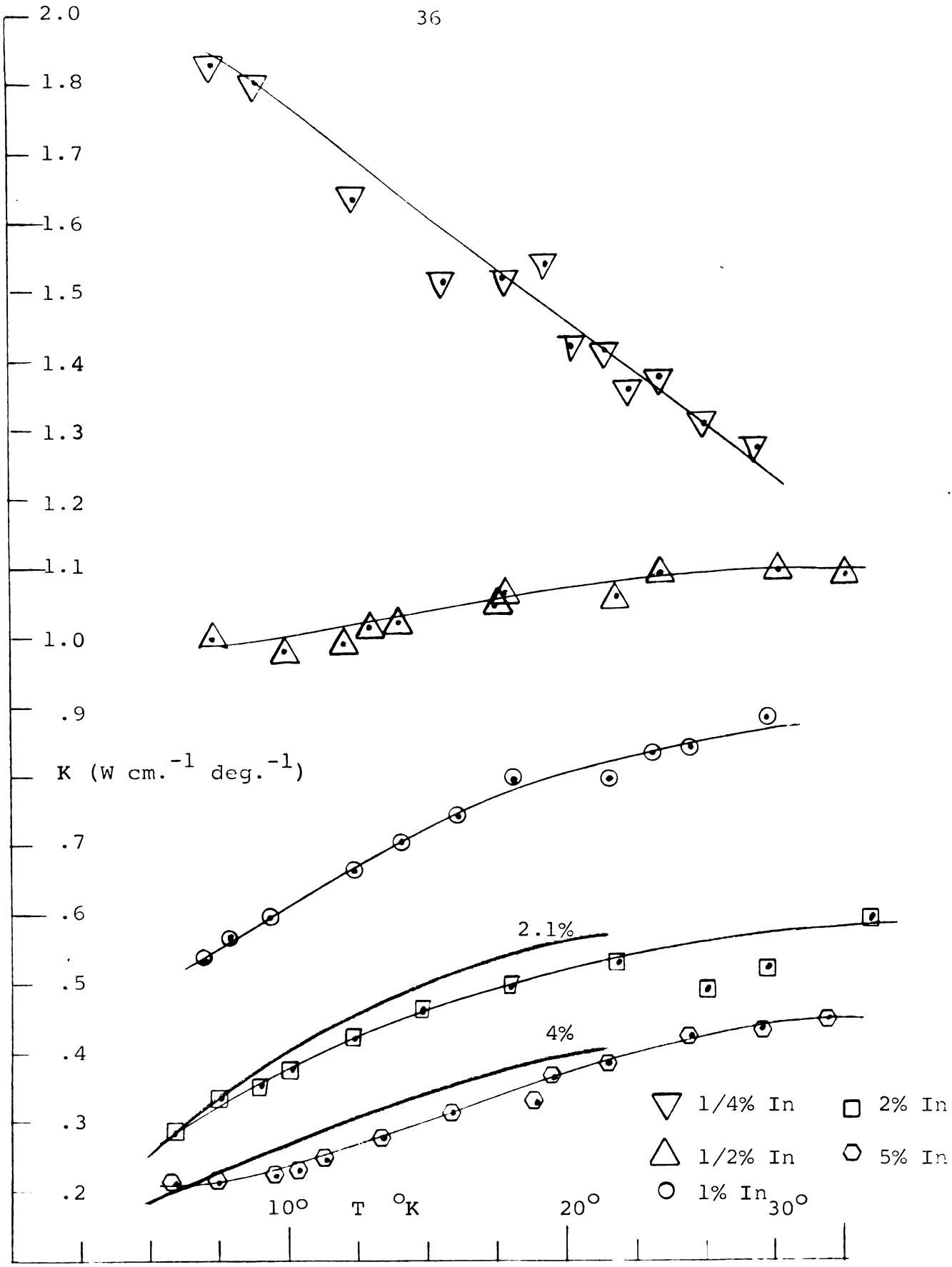

Figure 12. Thermal conductivity of tin-indium alloys.

the lattice term is no longer negligible. Fig. 13 shows this plot for the same data as in Fig. 12. The values of ρ_o/L_o measured are marked on the axis at zero degrees, and the extrapolation of the curves is also indicated. There was no minimum in the measured conductivity. However, the data suggests that such a minimum exists and that it shifts to higher temperature as the percent of solute increases. The dip in the curves at low temperatures ($\sim 10^{\circ}K$) is at least partially due to a lattice term, K_g. As the percent of solute is increased, the K_g term becomes a larger part of the total conductivity, and Eqn. 26 is no longer a good approximation.

For high concentration alloys, the ideal part of the electronic component, W_d, should be small enough to neglect. The conductivity will then be of the form of Eqn. 22, and K_e becomes $\frac{LT}{\rho}$:

$$K = \frac{LT}{\rho} + AT^2 \qquad \text{Eqn. 28.}$$

A plot of K/T against T for these results is shown in Fig. 14. At relatively high temperature and high concentrations, the measurements are approximately straight lines. The slope of these lines is either negative or zero, however, this corresponds to a negative or zero lattice conductivity: a physically unreal situation.

If the ideal resistivity is included in Eqn. 28, the result is:

$$\frac{K}{T} = \frac{1}{\frac{\rho_o}{L} + Bt^3} + AT \qquad \text{Eqn. 29.}$$

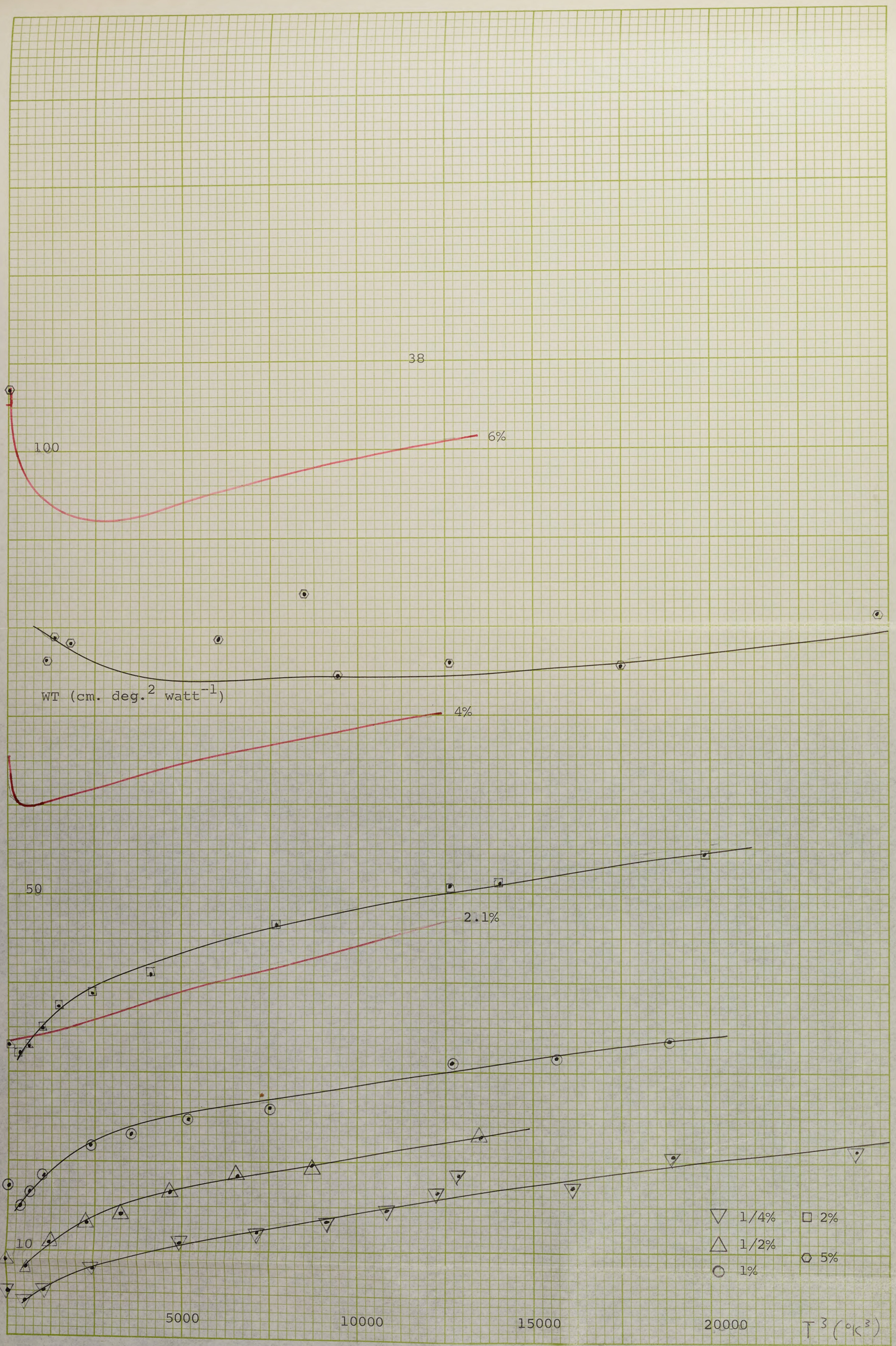

Figure 13. WT vs. T^3 for tin-indium alloys.

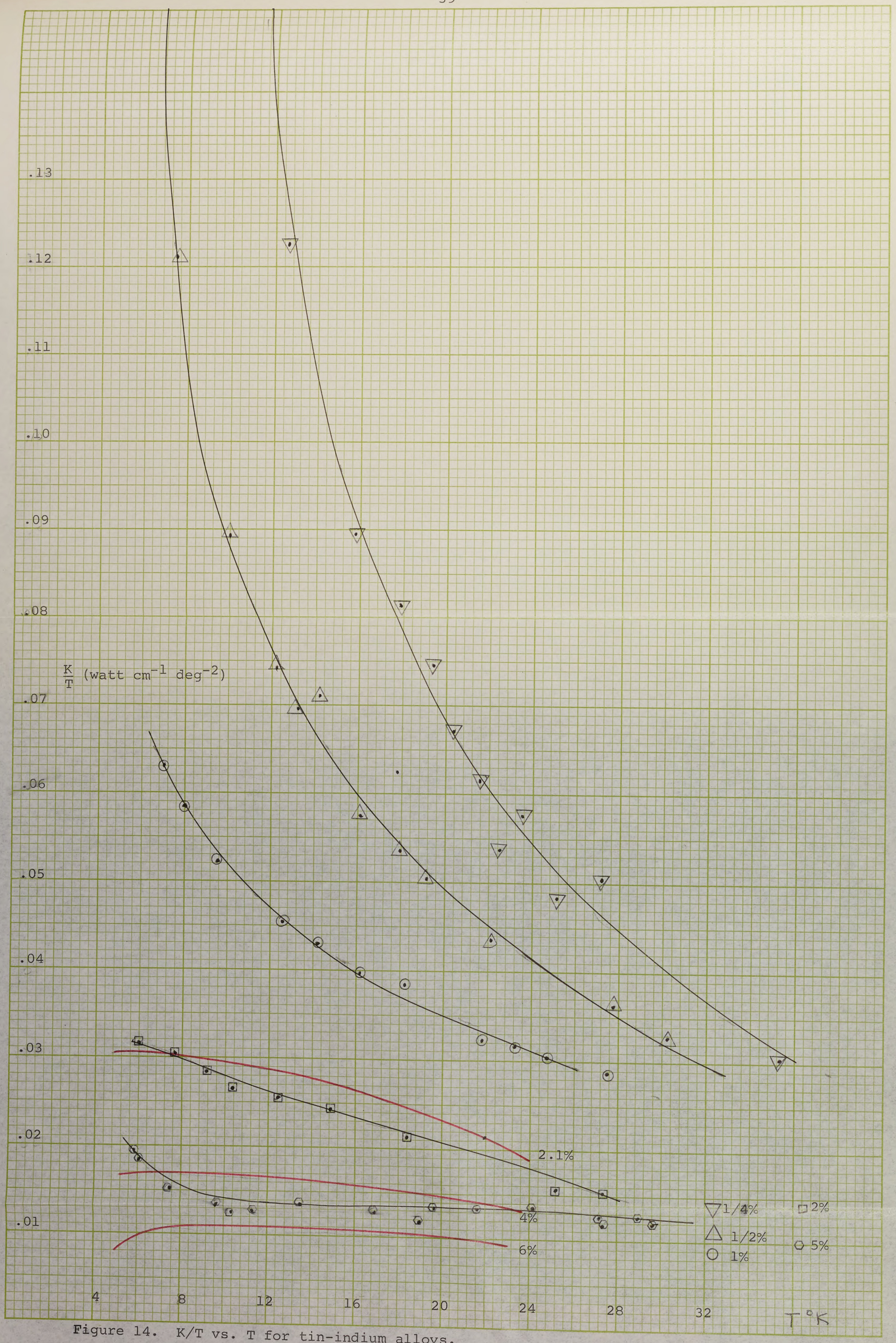

Figure 14. K/T vs. T for tin-indium alloys.

It is difficult to use this formula as a basis of analysis. Shiffman has simplified this by expanding the K_e term in Eqn. 29. This method cannot be used on our data, however, because the necessary approximation is not accurate for our samples. Another method of accounting for lattice, residual, and electronic resistivity is the following. The lattice thermal conductivity is obtained from Eqn. 22, where $K_e = \frac{1}{W_e}$ in Eqn. 26.

The value of W_o is obtained from the resistivity measurements. The ideal thermal resistance, W_o', can be obtained several ways. For the purpose of this analysis, however, W_i was calculated in the following way. Rosenberg (1955) measured the thermal conductivity of pure tin, and the purity of his sample was very nearly the same as ours. From his thermal resistance data, the residual thermal resistance, $\frac{\rho_o}{LT}$, was subtracted at several points between 10^o and 30^oK. The remainder was assumed to be W_i. Figure 15 shows the electronic thermal conductivity, K_e, in relation to the total conductivity. For one sample, K_g would be positive. However, the fact that the calculated electronic conductivity is larger than the total measured conductivity in the other samples indicates that: (1) There is a relatively large, unaccounted for error in some of the data, or (2) Eqn. 26 doesn't accurately describe these alloys.

The error in any quantity in Eqn. 27 is believed to be less than 2%. However, there is an error introduced

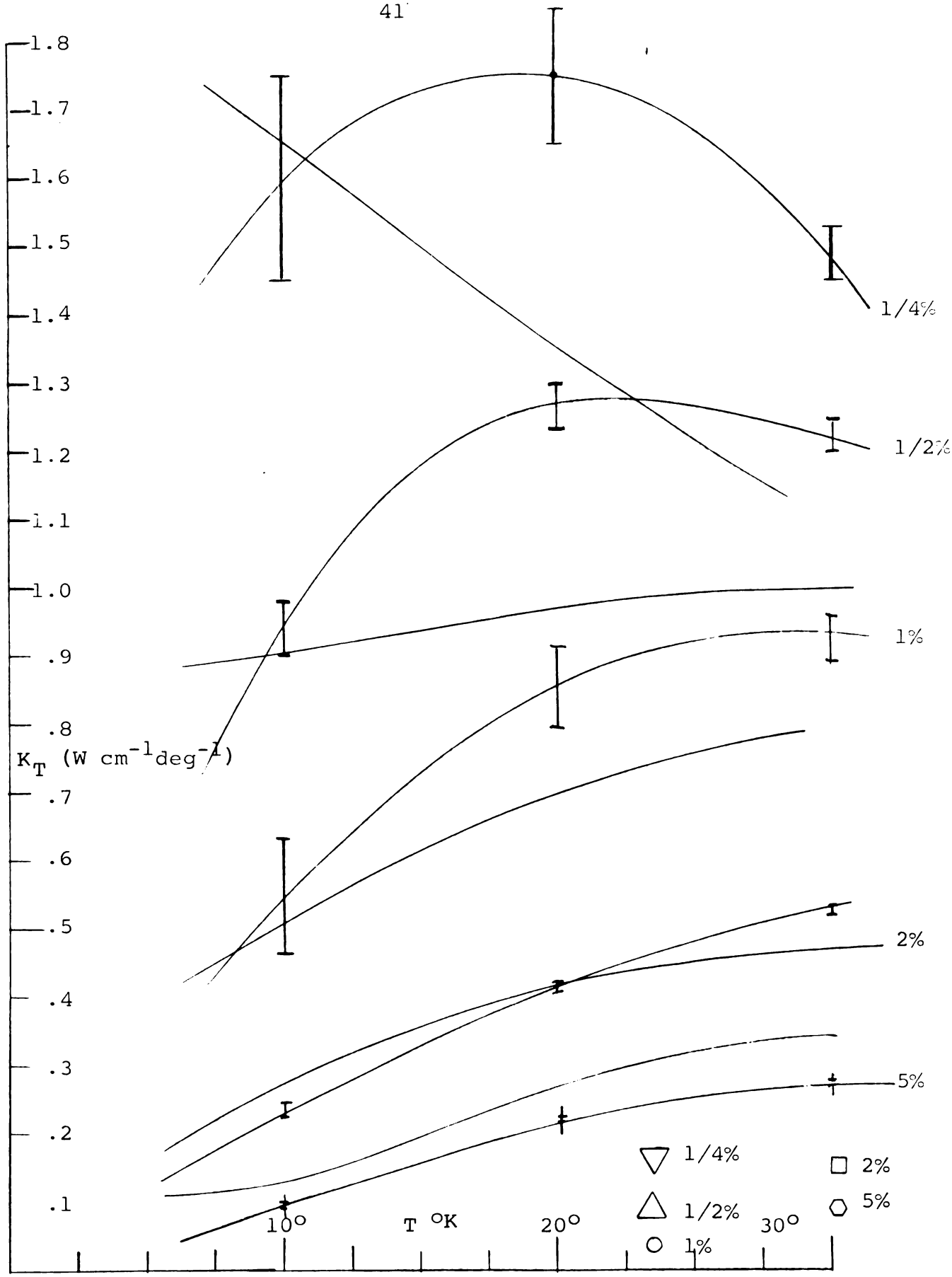

Figure 15. Total and electronic thermal conductivity of tin-indium alloys.

by the fact that, as the specific heat increases, the rate that the sample reaches thermal equilibrium decreases. Small random variations in the thermocouple EMF made the temperature change difficult to resolve when the sample was near equilibrium, and true equilibrium was not always attained. The estimated error from this source is approximately 3%-5%. Errors in the electronic thermal conductivity are indicated approximately in Fig. 15.

REFERENCES

Aleksandrov, V. N. and I. G. D'Yackov, Zh. eksper. theor. Fiz. (USSR) 43, No. 3(9)(1962).

Blatt, F. J., "Solid State Physics," 4, 225(1957).

Christian, J. W., Jan, J. P., Pearson, W. B., and Templeton, F. M., Proc. Roy. Soc. A 245, 213(1958).

Gantmakher, V. F., Soviet Phys. JETP 17, 549(1963).

Garber, M., Scott, B. W., and Blatt, F. J., Phys. Rev. 130, 2188(1963).

Gold, A. V., and Priestley, M. G., Phil. Mag. 5, 1089(1960).

Hansen, M., "Constitution of Binary Alloys," McGraw-Hill (1958).

Henry, W. G. and Schroeder, P. A., Can. J. Phys. 41, 1076 (1963).

Jones, H., "Encyclopedia of Physics," 28(1956).

Klemens, P. G., "Encyclopedia of Physics," 14 pt.4(1956).

Klemens, P. G., "Solid State Physics," 7, 1(1958).

Kohler, M., Z. Phys., 126, 481(1949).

Kunzler, J. E. and Renton, C. A., Phys. Rev. 108, 1397(1957).

MacDonald, D. K. C., Physica, 20, 996(1954).

Pullan, G. T., Proc. Roy. Soc. A 217, 280(1953).

Shiffman, C. A., Proc. Roy. Soc. 71, pt.4(1958).

Sondheimer, E. H., Proc. Roy. Soc. A 203, 75(1950).

Sondheimer, E. H., Can. J. Phys., 34, 1246(1956).

Wilson, A. W., "The Theory of Metals," 2nd Ed., Cambridge Univ. Press (1954).

Wolf, R. A., Thesis, Michigan State University (1963).

Ziman, J. M., Phil. Mag. Supplement 10, No. 37(1961).